Unsteady simulations of liquid/gas interfaces using the Second Gradient theory

A. Davy Nayigizente*, A. Thomas Schmitt, A. Sébastien Ducruix
Laboratoire EM2C, CNRS, CentraleSupélec, Université Paris-Saclay, France
davy.nayigizente@centralesupelec.fr, thomas.schmitt@centralesupelec.fr,
sebastien.ducruix@centralesupelec.fr

Abstract

The present work introduces a method to treat interfaces in a multiphase flow with phase changes using the so-called Second Gradient theory introduced by Van Der Waals (1789) and later extended by Cahn and Hilliard (1958). In the prospect of simulating a full cryogenic rocket-engine ignition, the model is intrinsically designed so as to treat such flows with real gas thermodynamics for a wide range of regimes, from a subcritical two-phase flow where the capillary dynamics pilot the system through the surface tension to a supercritical fluid where such effects disappear. Its thermodynamic consistency, a key element, has been thoroughly investigated and demonstrated using canonical mono-dimensional cases. In order to reach a reasonable grid resolution, an interface thickening method has been developed, inspired by the work of Jamet et al. (2001). It allows to keep a typical direct numerical simulation (from the turbulence point of view) resolution for the interface. This method has been implemented in the code AVBP, jointly developed by CERFACS and IFPEN, and validated on two-dimensional simulations of out-of-equilibrium plane interfaces. The model has been used to simulate liquid-gas mixing layer and is currently applied to non isothermal liquid jet injection.

Introduction

Current industrial propulsion devices operate over a wide range of temperature and pressure in the combustion chamber and systems such as rocket engines are likely to experience a severe change in thermodynamic regimes during ignition . In transcritical/supercritical conditions, the interactions between the fluid constituents no longer follow the assumptions of the ideal gas law and can no longer be neglected. The non-ideality of such fluids, referred to as real gases, is treated trough the usage of a proper equation of state (EoS) among which the cubic EoS, such as Soave-Redlich-Kwong (SRK) [1] see Fig. 1, have been extensively and successfully used in simulations [2, 3, 4, 5].

The treatment of subcritical regimes demands an additional model to deal with interface, phase change and capillary effects, such EoS being limited to transcritical/supercritical regimes. When it comes to simulating two-phase flows with phase change, two main categories can usually be considered. The sharp interface methods such as Level-Set [6], Volume-Of-Fluid [7] or Front-Tracking [8] consider the interface as a discontinuity and use jump conditions to treat the phase change. On the other hand, diffuse interface method such a Multi-Fluid [9, 10] or the Phase-Field [11, 12] consider the interface as a volumetric region where the thermodynamic variables vary rapidly yet continuously. A key point for all these methods is the proper transcription of the surface tension since this macroscopic quantity will have a strong impact on the interface behavior and in particular on the atomization regimes. The Convected-Distributed Force [13] and Continuum Surface Force [14] are the most commonly used methods to introduce surface tension in the previous models.

The Second Gradient theory, introduced by van der Waals [15], developed by Korteweg [16], Cahn & Hilliard [11] and completed by Germain [17] and [18] is a diffuse interface method where the density gradient, which takes great values in the interfacial zone, is used to modify the expression of the thermodynamic variables. The surface tension and phase change being naturally embedded in the model, it articulates well with real gas EoS and can be applied to compressible flows without additional treatment, motivating its use for our study. However, the model predicts interface widths multiple orders of magnitude below the smallest eddies due to turbulence making it non-affordable for a Direct Numerical Simulation (DNS) with an interface properly resolved. The purpose of this study is to propose a method to thicken an interface without modifying its key macroscopic features, in particular its surface tension.

The following outline is used in this document: section 2 offers a brief introduction to the native Second Gradient model and its main features; in section 3 we present the thickening strategy we use for our method along with a quick insight into its thermodynamic justification; finally section 4 offers some test cases and numerical results.

*Corresponding author: davy.nayigizente@centralesupelec.fr

Physical model

The Second Gradient theory is a consistent model which allows the description of a liquid-vapor interface. In this model, whose thermodynamics has been introduced by van der Waals [15], the interface is viewed as a continuous volumetric region of transition rather than a local discontinuity, which is consistent with the actual microscopic nature of an interface. The classical width and surface tension associated with a surfacic discontinuity can be related to a volumetric width and a volumetric excess energy due to the rapid yet continuous variation of the thermodynamic variables, in particular the density, caused by the presence of the interface.

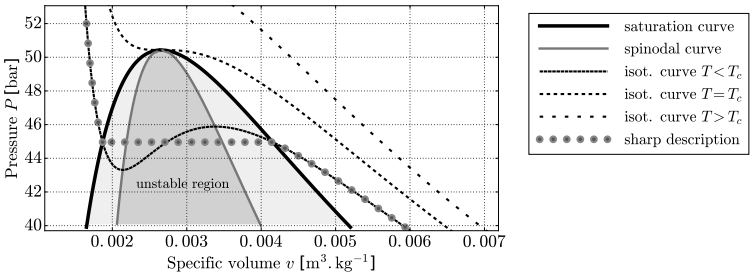

Figure 1: Clapeyron's diagram for pure oxygen O_2 with isothermal curves for different thermodynamic regimes using SRK-EoS [1]

Thermodynamic description

The thermodynamic description has been first expressed by [15] for pure fluids and later extended by [11] to non-miscible binary fluids. In the interfacial region, the strong density gradient can no longer be neglected and has to be considered in the description of the thermodynamic variables. This modification is first applied to the volumetric free energy F, which can be written in this new model:

$$F\left(T,\rho,\boldsymbol{\nabla}\rho\right)=F^{\text{EoS}}\left(T,\rho\right)+\frac{\lambda\left(T\right)}{2}\left(\boldsymbol{\nabla}\rho\right)^{2} \tag{1}$$

where T and ρ are the fluid temperature and density, F^{EoS} is the volumetric free energy given directly by the EoS and λ is the capillary coefficient, a temperature dependent parameter who will be shown to drive the behavior of the interface at equilibrium (the interested reader can find more details of its calculation in [19]) In this study, λ will be assumed independent of the temperature and the impact of this hypothesis is discussed in [10]. Overall, this modification leads to a new Gibbs equation :

$$de_s=T\,ds+\frac{P_{\text{th}}}{\rho^2}\,d\rho+\frac{\lambda}{\rho}\boldsymbol{\nabla}\rho\cdot d\boldsymbol{\nabla}\rho \tag{2}$$

and also impacts other thermodynamics variables such as the thermodynamic pressure P or the specific sensible energy e_s and the chemical potential μ as follows:

$$P_{\text{th}}=P^{\text{EoS}}-\frac{\lambda}{2}\left(\boldsymbol{\nabla}\rho\right)^{2} \tag{3}$$

$$e_s=e_s^{\text{EoS}}+\frac{\lambda}{2\rho}\left(\boldsymbol{\nabla}\rho\right)^{2} \tag{4}$$

$$\mu=\mu^{\text{EoS}} \tag{5}$$

where the superscript $*^{\text{EoS}}$ refers to the corresponding thermodynamic variable as given by the chosen EoS.

This added dependency on $\boldsymbol{\nabla}\rho$ allows to stabilize the thermodynamics in the binodal region otherwise known to be unstable when using native real gas EoS. Without the contribution from the Second Gradient, reaching a point in this region leads to a spinodal decomposition of the fluid between liquid and vapor phases and to a sharp interface description [20].

Mechanical description

It is demonstrated in [21] that the apparent instability of the spinodal region arises from a lack of precision in the description of the molecular interactions occurring inside the interfacial region. A development of the intermolecular potential in that region leads to a new expression of the internal pressure tensor that presents a strong

anisotropy. This result has also been shown by [16] by deriving the momentum equation of such a fluid introducing a new pressure tensor. The full set of fluid motion equations can be derived, along with the thermodynamics and from [12] it writes:

$$\frac{\partial \rho}{\partial t} = -\boldsymbol{\nabla} \cdot \rho \mathbf{v} \tag{6a}$$

$$\frac{\partial \rho \mathbf{v}}{\partial t} = -\boldsymbol{\nabla} \cdot \left[\rho \mathbf{v} \otimes \mathbf{v} + p\underline{\underline{\mathbf{I}}} + \lambda \boldsymbol{\nabla}\rho \otimes \boldsymbol{\nabla}\rho - \underline{\underline{\boldsymbol{\tau}}}^d\right] \tag{6b}$$

$$\frac{\partial \rho e}{\partial t} = -\boldsymbol{\nabla} \cdot \left[(\rho e + p)\,\mathbf{v} + \lambda\,(\boldsymbol{\nabla}\rho \otimes \boldsymbol{\nabla}\rho) \cdot \mathbf{v} + \lambda\rho\boldsymbol{\nabla}\rho\,(\boldsymbol{\nabla} \cdot \mathbf{v}) - \underline{\underline{\boldsymbol{\tau}}}^d \cdot \mathbf{v} + \boldsymbol{q}\right] \tag{6c}$$

where $\mathbf{v}$ is the velocity of the fluids, e the total specific energy sum of the specific sensible energy e_s and the specific kinetic energy $e_c = \mathrm{v}^2/2 = |\mathbf{v}|^2/2$, p is the mechanical pressure given by

$$p = P^{\text{EoS}} - \frac{\lambda}{2}(\boldsymbol{\nabla}\rho)^2 - \rho\boldsymbol{\nabla} \cdot (\lambda\boldsymbol{\nabla}\rho) \tag{7}$$

and stands as the isotropic part of the pressure tensor, $\underline{\underline{\boldsymbol{\tau}}}^d$ and $\boldsymbol{q}$ are the viscous constraints vector and the heat flux. From now on, both diffusive fluxes will be omitted, restraining the system to capillary-Euler equations.

Macroscopic variables

This theory also allows a natural definition of the surface tension σ as it corresponds to the excess volumetric free energy between the diffuse interface profile obtained with the Second Gradient and discontinuous interface profile from the sharp interface methods as shown Fig. 2. By noting F and F_{sh} the associated volumetric free energy profile for a one-dimensional planar isothermal interface between the pure vapor and pure liquid boundaries x_v and x_l, σ is defined by:

$$\sigma = \int_{x_v}^{x_l} \left(F\left(x\right) - F_{\text{sh}}\left(x\right)\right) dx \tag{8}$$

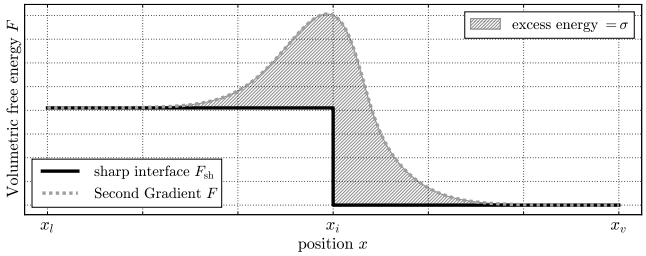

Figure 2: Representation of the excess volumetric free energy for a 1d planar interface

Using thermodynamic arguments as in [11] or mechanical development as in [12] and one can show that σ can also be linked to the thermodynamic description of the fluid through its chemical potential by:

$$\sigma = \int_{x_v}^{x_l} \left[2 \int_{\rho_v}^{\rho(x)} \left(\mu^{\text{EoS}} - \mu^{\text{sat}}\right)(\varrho)\, d\varrho\right] dx \tag{9}$$

where μ^{sat} is the chemical potential given by the EoS at saturation, known to be the same in both bulk phases.

One can also define the interface thickness and though this definition is not unique, Eq. (10) has a practical understanding in terms of how well the density gradients are resolved on a given mesh:

$$h = \frac{(\rho_l - \rho_v)}{\max|\boldsymbol{\nabla}\rho|} \tag{10}$$

Based on thermodynamic arguments, not developed here, one can give the dependency of the interface width

and the surface tension σ with the capillary coefficient λ:

$$\begin{aligned} h &\propto \sqrt{\lambda} \\ \sigma &\propto \sqrt{\lambda} \end{aligned} \tag{11}$$

First validations

The behavior of the model has been tested in one dimension on isothermal interfaces to test its thermodynamic accuracy and robustness. When applied to interfaces at equilibrium, the following features of the model, as expected, were properly observed: the saturation densities ρ_v and ρ_l for a given temperature are retrieved (by comparing them to values based on thermodynamic equilibrium considerations); the interface has a defined width impacted by the temperature and the capillary coefficient; no interface is observed once the critical temperature is exceeded. In dynamic conditions, the interface is properly convected and returns to its equilibrium profile if an initial deformation (stretching/compression) has been initially applied upon it.

Thickened Interface Method

Notwithstanding its thermodynamic accuracy, the Second Gradient theory in its native form suffers a lack of applicability for practical systems since a slight descent under the critical temperature promptly leads to very small interface thicknesses, around a few nm for pure oxygen for instance. On the other hand, the typical Kolmogorov's scale of the smallest eddies for our typical flows (like liquid rocket-engines or Diesel engines) lies within a few μm. The relative scale between the eddies' size and the interface width, easily around 10^3 to 10^5, asks for, among other possible strategies, a method to artificially thicken the interface, even to reach the so-called DNS meshes that the turbulence is resolved on. The following section offers a method to achieve this thickening complying to both physical consistency and practical applicability.

Derivation of the method

Several methods have already been suggested in order to achieve interface thickening. Indeed, as observed in [10] and from Eq. (11), increasing the capillary coefficient λ would thicken the interface but would also modify surface tension and therefore a lead to a modified macroscopic behavior. However, using a specific analytical form for the density profile, justified near the critical point, Jamet in [12] showed in a first method the possibility to act simultaneously on the surface tension and the interface width using two coefficients. To get a wider range of applicability, he developed a second method where the thermodynamics was carefully altered in the binodal region so as to thicken the interface while maintaining a thermodynamic consistency, arguably at the expense of computational complexity and cost [12], [22]. Inspired by these two methods, we derive a new method trying to mix their respective advantages. Eq. (9) hints that the chemical potential must be modified in the binodal region while the interface is being thickened to counteract the augmenting effect of the capillary coefficient. More precisely, the quantity $\mu^{\text{EoS}} - \mu^{\text{sat}}$ should be diminished, for instance dividing it by a given coefficient, referred to as ϕ_s in this study. The new non-capillary chemical potential μ^{TIM} is expressed as:

$$\mu^{\text{TIM}}(\rho, T) = \mu^{\text{sat}}(T) + \frac{\mu^{\text{EoS}}(\rho, T) - \mu^{\text{sat}}(T)}{\phi_s} \tag{12}$$

To ensure thermodynamic consistency, the expression of the other non-capillary variables must be derived using thermodynamic relations such as the Gibbs equation and Maxwell rules, the complete derivation can be found in in [23]. Noticeably, the new non-capillary thermodynamic pressure P^{TIM}, specific sensible energy ${e_s}^{\text{TIM}}$ and entropy s^{TIM} are expressed by:

$$P^{\text{TIM}}(\rho, T) = P^{\text{sat}}(T) + \frac{P^{\text{EoS}}(\rho, T) - P^{\text{sat}}(T)}{\phi_s} \tag{13}$$

$${e_s}^{\text{TIM}}(\rho, T) = {e_s}^{\text{sat}}(T) + \frac{{e_s}^{\text{EoS}}(\rho, T) - e^{\text{sat}}(T)}{\phi_s} + \left(1 - \frac{1}{\phi_s}\right)\xi(\rho, T) \tag{14}$$

$$s^{\text{TIM}}(\rho, T) = s^{\text{sat}}(T) + \frac{s^{\text{EoS}}(\rho, T) - s^{\text{sat}}(T)}{\phi_s} + \left(1 - \frac{1}{\phi_s}\right)\Psi(\rho, T) \tag{15}$$

where ξ and Ψ are functions such as $\lim_{\rho \to \rho_l,\ \rho_v} \Psi(\rho, T) = 0$ and $\lim_{\rho \to \rho_l,\ \rho_v} \xi(\rho, T) = 0$ ensuring the continuity of ${e_s}^{\text{TIM}}$ and s^{TIM} trough the binodal region. Finally, the method uses two coefficients ϕ^l and ϕ_s to simultaneously thicken the interface using a greater capillary coefficient while impending the augmentation of the surface tension.

The modifications are applied as follow:

$$P^* = P^{\text{TIM}} \quad \text{in the binodal region} \qquad P^* = P^{\text{EoS}} \quad \text{otherwise} \tag{16}$$

$$e_s{}^* = e_s{}^{\text{TIM}} + \frac{\lambda^*}{2\rho}\left(\boldsymbol{\nabla}\rho\right)^2 \quad \text{in the binodal region} \qquad e_s{}^* = e_s{}^{\text{EoS}} + \frac{\lambda^0}{2\rho}\left(\boldsymbol{\nabla}\rho\right)^2 \quad \text{otherwise} \tag{17}$$

$$\lambda^* = \phi^l \lambda^0 \quad \text{in the binodal region} \qquad \lambda^* = \lambda^0 \quad \text{otherwise} \tag{18}$$

λ^0 is the reference capillary coefficient of the non modified interface. Consequently, the new total specific energy is given by $e^* = e_s{}^* + e_c$. The restriction of the modifications applied on thermodynamic variables and λ ensures that the stability of the bulk phases will not be jeopardized. The resulting capillary-Euler equations are:

$$\frac{\partial \rho}{\partial t} = \boldsymbol{\nabla} \cdot [\rho \mathbf{v}] \tag{19a}$$

$$\frac{\partial \rho \mathbf{v}}{\partial t} = -\boldsymbol{\nabla} \cdot \left[\rho \mathbf{v} \otimes \mathbf{v} + P^* + \lambda^* \Big[-\big(\frac{1}{2}(\boldsymbol{\nabla}\rho)^2 + \rho \boldsymbol{\nabla} \cdot (\boldsymbol{\nabla}\rho)\big) \underline{\underline{I}} + (\boldsymbol{\nabla}\rho \otimes \boldsymbol{\nabla}\rho) \Big] \right] \tag{19b}$$

$$\frac{\partial \rho e^*}{\partial t} = -\boldsymbol{\nabla} \cdot \left[\left(\rho e^* + P^*\right) \mathbf{v} + \lambda^* \Big[-\big(\frac{1}{2}(\boldsymbol{\nabla}\rho)^2 + \rho \boldsymbol{\nabla} \cdot (\boldsymbol{\nabla}\rho)\big) \mathbf{v} + + \nabla\rho \left(\boldsymbol{\nabla} \cdot (\rho \mathbf{v})\right) \Big] \right] \tag{19c}$$

If the coefficients are chosen such as $\phi_s = \phi^l = \mathrm{F}$, the interface is thickened by a factor F without modifying the value of its surface tension.

First validation of the method

The Thickened Interface Method (TIM) has been validated on one-dimensional configurations by successfully replicating the test cases from for different values of the thickening factor ranging from $\mathrm{F} = 1$ to $\mathrm{F} = 1000$. It has also been validated on two-dimensional configurations by studying the oscillation period of planar interfaces to which a harmonic initial deformation has been applied following the study in [24]. The corresponding in results can be found in [23].

Test cases and results

Numerical setup

In this section, we present the different test cases computed using the TIM. These calculations have been performed using the solver AVBP jointly developed by CERFACS and IFPEN (see [25, 26] among others) in its real-gas version developed with the help of EM2C (AVBP-RG see [27]) who has already been successfully used to perform simulations of cryogenic rocket engine under supercritical conditions in DNS [28] and mostly LES [3, 5]. The scheme used relies on a third order Galerkin finite-element spacial discretization and a second order Runge-Kutta time integration. A conservative selective filter is applied to remove high order spurious oscillations. Therewith, AVBP relies on the characteristic waves approach from [29] to treat the boundaries.

Test cases design

The fluid considered is pure nitrogen. The studied case is that of a symmetrical mixing layer that take the aspect of a liquid jet in its own vapor. The surrounding vapor is initially at rest whereas the liquid has a constant descending vertical velocity v_l. The simulations are performed on a regular cartesian mesh. The domain is periodic vertically and non-reflecting boundary conditions are used on the left and right boundaries. The useful parameters of the simulation as recalled in Tab. 1 where D is the jet diameter, h the interface width, N the number of points in the gradient, N_x, N_y are the number of points in x and y directions and L_x, L_y are the corresponding lengths.

While the density, pressure and temperature profiles are the same for all cases, two different values have been used for the liquid velocity so as to get two different Weber numbers $We = \rho_v \mathrm{v}_l^2 D/\sigma$ typical of three different atomization regimes (see [30]): $\mathrm{v}_1 = 17.9$ m/s for $We_1 = 50$, $\mathrm{v}_2 = 25.4$ m/s for $We_2 = 100$ and $\mathrm{v}_3 = 35.9$ m/s for $We_3 = 200$.

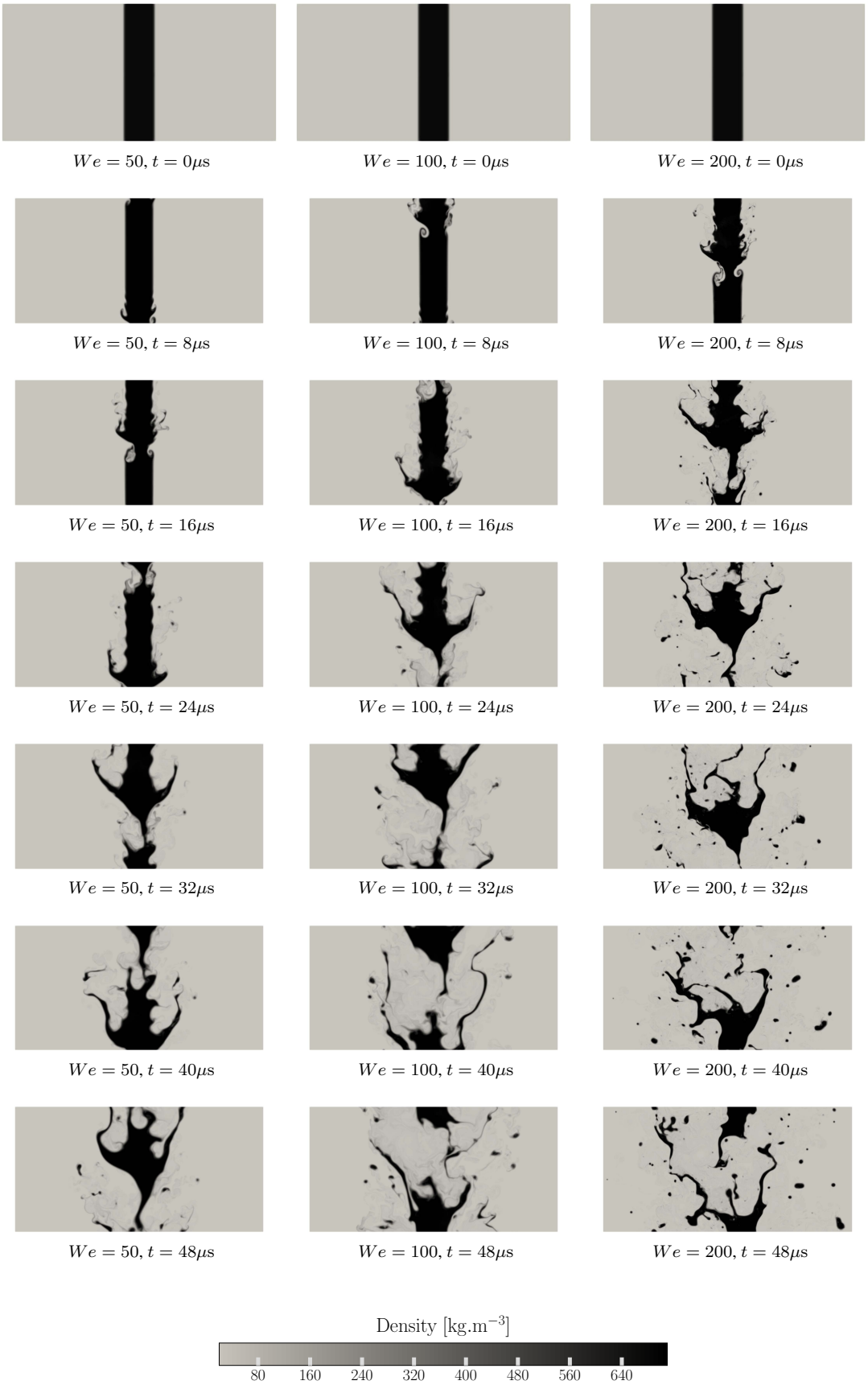

Figure 3: Evolution in time of the density profiles for two-dimensional periodic Nitrogen liquid jets in their vapor

Table 1: Simulation parameters

T_0	λ_0	F	σ	$L_y = L_x/2$	$N_y = N_x/2$	$\Delta_x = \Delta_y$	h	D	N
100.0 K	19.6 $\mathrm{mm}^7/\mathrm{g}/\mathrm{s}^2$	1000	4.134 mN/m	90.0 μm	675	0.133 μm	1.31 μm	20.0 μm	≈ 9

Discussion

For $We_1 = 50$, the jet faces a strong macroscopic deformation with no clear breakup as expected for a regime between the Rayleigh non-axisymmetric and the shear breakup, see [31]. Macroscopic structures tend to form and can be expected to eventually separate and coalesce to form a small number of big droplets. The case $We_3 = 200$ shows a great modification of the jet topology. Long macroscopic ligaments can be observed to form and break-up quickly to form droplets among which the biggest also tend to experience a secondary break-up. This is reminiscent of the membrane regime [31]. In-between, the case $We_2 = 100$ also displays macroscopic ligament, droplets are generated but quickly absorbed by coalescence in the larger structures. These observations are consistent with a regime between the shear breakup and the membrane regimes. Overall, the three test cases qualitatively display the expected behaviors in agreement with experimental studies.

Conclusions and prospects

This study has introduced the Thickened Interface Method as a solution to perform simulations of interfaces on typical DNS meshes using the Second Gradient model. The modifications applied to the model have been presented along with a brief thermodynamic justification. The method showed good agreements with typical test cases found in the literature and two-dimensional cases of subcritical jets where classical atomization regimes have been properly retrieved. The method has been derived and tested for isothermal cases and though its application to non-isothermal cases is promising, its impact is still under investigation. The mathematical characterization of the system of equations is of also primary interest as it would allow the derivation of proper boundary conditions and the use of more robust numerical scheme. Finally, the extension to multispecies mixtures should allow first test cases on realistic systems such as rocket and Diesel engines.

Acknowledgements

The authors acknowledge funding from ANR through project ANR-14-CE22-0014 (SUBSUPERJET). The authors also warmly thank M. Pelletier from EM2C laboratory for insightful discussions.

References

[1] Soave, G.: Equilibrium constants from a modified Redlich-Kwong equation of state. *Chemical Engineering Science* **27**(6), 1197:1203 (1972).

[2] Oefelein, J.C.: Mixing and combustion of cryogenic oxygen-hydrogen shear-coaxial jet flames at supercritical pressure. *Combustion Science and Technology* **178**(1-3), 229:252 (2006)

[3] Schmitt, T., Selle, L., Ruiz, A., Cuenot, B. *Large-eddy simulation of supercritical-pressure round jets*. AIAA journal **48**(9), 213:2144 (2010)

[4] Schmitt, T., Méry, Y., Boileau, M., Candel, S.: Large-eddy simulation of oxygen/methane flames under transcritical conditions. *Proceedings of the Combustion Institute* **33**(1), 1383:1390 (2011)

[5] Urbano, A., Selle, L., Staffelbach, G., Cuenot, B., Schmitt, T., Ducruix, S., Candel, S. *Exploration of combustion instability triggering using large eddy simulation of a multiple injector liquid rocket engine*. Combustion and Flame **169**, 129:140 (2016)

[6] Olsson, E., Kreiss, G., Zahedi, S.: A conservative level set method for two phase flow II. *Journal of Computational Physics* **225**(1), 785:807 (2007)

[7] Hirt, C.W., Nichols, B.D.: Volume of fluid (vof) method for the dynamics of free boundaries. *Journal of Computational Physics* **39**(1), 201:225 (1981)

[8] Tryggvason, G., Bunner, B., Esmaeeli, A., Juric, D., Al-Rawahi, N., Tauber, W., Han, J., Nas, S., Jan, Y.J.: A front-tracking method for the computations of multiphase flow. *Journal of Computational Physics* **169**(2), 708: 759 (2001).

[9] Allaire, G., Clerc, S., Kokh, S.: A five-equation model for the simulation of interfaces between compressible

fluids. *Journal of Computational Physics* **181**(2), 577:616 (2002).
[10] Gaillard, P.: Interfaces diffuses et flammes transcritiques lox/h2. *Ph.D. thesis*, Université Pierre et Marie Curie- Paris VI (2015)
[11] Cahn, J.W., Hilliard, J.E.: Free energy of a nonuniform system. i. interfacial free energy. *Journal of Chemical Physics* **28**(2), 258:267 (1958).
[12] Jamet, D.: Etude des potentialités de la théorie du second gradient pour la simulation numérique directe des écoulements liquide-vapeur avec changement de phase. *Ph.D. thesis*, Ecole Centrale Paris (1998)
[13] Unverdi, S.O., Tryggvason, G.: A front-tracking method for viscous, incompressible, multi-fluid flows. *Journal of Computational Physics* **100**(1), 25:37 (1992)
[14] Brackbill, J.U., Kothe, D.B., Zemach, C.: A continuum method for modeling surface tension. *Journal of Computational Physics* **100**(2), 335:354 (1992).
[15] van der Waals, J.D.: The thermodynamic theory of capillarity under the hypothesis of a continuous variation of density. *Journal of Statistical Physics* **20**, 200:244 (1979).
[16] Korteweg, D.J.: Sur la forme que prennent les équations du mouvement des fluides si l'on tient compte des forces capillaires causées par des variations de densité considérables mais continues et sur la théorie de la capillarité dans l'hypothèse d'une variation continue de la densité. *Archives Néerlandaises des Sciences exactes et naturelles* **6**(1), 265 (1901)
[17] Germain, P.: Sur l'application de la méthode des puissances virtuelles en mécanique des milieux continus. *Comptes rendus hebdomadaire de l'Académie des Science A* **274**(22), 1051:1055 (1972)
[18] Seppecher, P.: Etude d'une modélisation des zones capillaires fluides: interfaces et lignes de contact. *Ph.D. thesis*, Ecole Nationale Supérieure de Techniques Avancées (1987)
[19] Lin, H., Duan, Y.Y., Min, Q.: Gradient theory modeling of surface tension for pure fluids and binary mixtures. *Fluid Phase Equilibria* **254**(12), 75:90 (2007).
[20] Carey, V.: Liquid Vapor Phase Change Phenomena: An Introduction to the Thermophysics of Vaporization and Condensation Processes in Heat Transfer Equipment, Second Edition. Taylor & Francis (2007).
[21] Rocard, Y.: Thermodynamique. Masson et Ode (1952).
[22] Jamet, D., Lebaigue, O., Coutris, N., Delhaye, J.: The second gradient method for the direct numerical simulation of liquid-vapor flows with phase change. *Journal of Computational Physics* **169**(2), 624:651 (2001)
[23] Nayigizente, D., Schmitt, T., Ducruix, S.: Development of an interface thickening method for the direct numerical simulation of compressible liquid-vapor flows in the framework of the Second Gradient theory. *Journal of Multiphase Flow* (2018)
[24] Fyfe, D., Oran, E., Fritts, M.: Surface tension and viscosity with lagrangian hydrodynamics on a triangular mesh. *Journal of Computational Physics* **76**(2), 349:384 (1988).
[25] Gourdain, N., Gicquel, L., Montagnac, M., Vermorel, O., Gazaix, M., Staffelbach, G., Garcia, M., Boussuge, J., Poinsot, T.: High performance parallel computing of flows in complex geometries: I. methods. *Computational Science & Discovery* **2**(1), 015,003 (2009)
[26] Moureau, V., Lartigue, G., Sommerer, Y., Angelberger, C., Colin, O., Poinsot, T.: Numerical methods for unsteady compressible multi-component reacting flows on fixed and moving grids. *Journal of Computational Physics* **202**(2), 710:736 (2005)
[27] Schmitt, T.: Simulation des grandes échelles de la combustion turbulente Ã pression supercritique. *Ph.D. thesis*, Toulouse INPT (2009)
[28] Ruiz, A. M., Lacaze, G., Oefelein, J. C., Mari, R., Cuenot, B., Selle, L., Poinsot, T. *Numerical benchmark for high-Reynolds-number supercritical flows with large density gradients*. AIAA Journal **54**(5), 1445:1460 (2015).
[29] Poinsot, T.J., Lele, S.K.: Boundary conditions for direct simulations of compressible viscous flows. *Journal of Computational Physics* **101**, 104:129 (1992).
[30] Lasheras, J., Hopfinger, E.: Liquid jet instability and atomization in a coaxial gas stream. *Annual Review of Fluid Mechanics* **32**(1), 275:308 (2000)
[31] Baillot, F., Blaisot, J.B., Boisdron, G., Dumouchel, C.: Behaviour of an air-assisted jet submitted to a transverse high-frequency acoustic field. *Journal of Fluid Mechanics* **640**, 305:342 (2009).